Field-evaporation kinetics (pulsed regime)

A. F. Bobkov and A. L. Suvorov

Institute of Theoretical and Experimental Physics
(Submitted 14 March 1980)
Zh. Eksp. Teor. Fiz. **79**, 1376–1384 (October 1980)

Results are presented of a field-ion microscopy analysis of the kinetics of pulsed (atom-by-atom) field evaporation of tungsten samples, both defect-free and containing crystal-structure defects. Values are obtained of the effective polarizabilty of surface atoms on the edges of the {112} planes ($\alpha_{\text{eff}} \approx 3.0$ Å^3), of the distances from the surface, at which field evaporation of ions with different charges takes place (from 0 to 0.8 Å for $n = 1$ to 3), and for the critical field intensity ($F_k \approx 6.17$ V/Å) at which the evaporation rate reaches a maximum. A qualitative mechanism of field evaporation in fields of medium strength ($F = F_{ev} \approx 5.7$ V/Å for tungsten) and high strength ($F \sim F_k = 6.17$ V/Å) is proposed. The advantages of using pulsed field evaporation (compared with the continuous regime) are demonstrated for use in the analysis of the defect structure of metals.

PACS numbers: 79.70. + q, 61.70. − r, 61.16.Fk

INTRODUCTION

Evaporation with the aid of a field, first discovered using a field ion microscope,[1] plays an indispensable role as a most important technique, in field-ion microscopy. It is at the same time of independent scientific interest. It is known that this phenomenon is realized in two regimes: continuous and pulsed. The former calls for maintaining at the metallic-sample surface an electric field of intensity exceeding the evaporation field F_{ev} (the start of field evaporation, see, e.g., Table I of Ref. 2) for a time much longer than the time of evaporation of a single surface atom $\Delta t \approx k_{ev}^{-1}$ (k_{ev} is the evaporation-rate constant[3,4]). The second regime is realized when the indicated times are of the same order of magnitude. An experimental investigation of the field-evaporation kinetics yields information on the details of the mechanism of the process and on some of its parameters, and reveals the most beneficial sample surface treatment for field-ion-microscopy analysis (see, e.g., Refs. 5–11). Most useful in the interpretation of the experimental data is simulation of the field evaporation process with a computer.[9,12] The pulsed field-evaporation method has in addition two other important methodological applications: in probe analysis of the chemical nature of individual particles and small complexes on the surface of a sample,[13,14] and in the analysis (study) of the defect structure of metals. The latter pertains in particular to solitary point defects[15] and to the point structure of pores and depleted zones. As shown earlier,[16,17] continuous field evaporation of the sample material leads not only to additional corrosion of the pores that emerge to the surface and hence to an artificial increase of their dimensions, but also, under previously determined conditions,[17,18] to a qualitative regeneration of the defects—depleted zones and pores. The use of pulsed field evaporation gets around these difficulties to a considerable degree.

The present study, a continuation of our earlier work,[9] was aimed at analyzing the character of pulsed field evaporation of tungsten samples, both defect-free and containing crystal-structure defects. The choice of the faces for the analysis ({112}) was dictated by the fact that it is precisely on these faces that we identified most frequently individual point defects[19] and dislocations[20] in our systematic investigation of radiation damage in metals.[21]

EXPERIMENTAL PROCEDURE AND RESULTS

All the experiments were performed with the instruments and apparatus described in Ref. 9. The pulsed field evaporation was produced using a high-voltage pulse generator with amplitude ΔU ranging from 230 to 4600 V (adjustable in steps of 100 to 800 V) and duration Δt from 0.1 to 10 μsec (in steps of 0.1 μsec). The investigation procedure ensured production of a stable ion-emission image of the surface of the tip (at a best surface-image voltage U_0) and its photography, application of the evaporating pulse with specified parameters (rise time Δt for a tip potential rise ΔU), repeated photography of the image, etc. Just as in our preceding study, the investigated samples were made of technically pure tungsten of VA-3 brand.

We note that even the determination of the field-evaporation parameters (let alone the analysis of the material crystal-structure defects) by using the pulsed regime offers certain advantages over the continuous regime. The reason is the negligibly small change of the average electric field intensity at the surface of the tip before and after one evaporating pulse. Since, however, the field-evaporation process has a probabilistic character, the measurements of low evaporation rates (one or several atoms per second) will be subject to a much larger error than in the case of measurement of higher (by several orders of magnitude) evaporation rates. At the same time experiments at high evaporation rates do not reveal such interesting effects as, e.g., the existence, observed in Refs. 9 and 10, of metastable configurations of atoms in the plane, the dependence of the "lifetimes" of the atoms in such configuration on the surface of the sample on the linear dimensions of the configurations, and the like.

The field-evaporation rate k_{ev} was determined in the present study (as in most others) by directly counting the number n_a of the atoms removed from the edges of the two upper planes in a single evaporation pulse: k_{ev}

 0038-5646/80/100695-05$02.40

TABLE I.

F, B/Å	k_{ev}, atom/μsec	$\ln \frac{k_{ev}(F)}{k_{ev}(F_{ev})}$
5.68	0.4±0.2	0
5.73	3.0±2.0	2.0
5.90	10.9±3.9	3.3
6.05	13.3±8.8	3.5
6.19	33.6±10.3	4.4

$=n_a/\Delta t$ atom/μsec. We take it into account here that this definition is arbitrary and does not make full allowance for the difference between the coordinations of the evaporating ions on the surface of the tip.

In the calculation of the evaporation-field intensity we used the empirical formula[3]

$$F=(U_0+\Delta U)/\beta R_0. \quad (1)$$

The local radius R_0 of the tip was determined from the number of the imaged crystal-plane edges between the two poles, and the geometric factor β was determined considering the fact that the field intensity for the best surface image corresponds to the conditions for field ionization of helium and amounts to 4.4 V/Å.

The pulsed field evaporation showed itself on the ion-microscope screen in different manners: in some cases a single evaporation pulse removed individual edge atoms, in others it removed the entire outer ring of the plane, and in still others, finally, a "collective" removal (simultaneous within the time interval Δt) of the atoms of the entire upper plane was observed.

Data representing the dependence of the field-evaporation rate k_{ev} on the electric field intensity F, calculated from series of field-emission images of non-irradiated tungsten are gathered [for the (112) face] in Table I. It is seen from this table that the weakest field at which signs of evaporation of the (112) plane of tungsten can be observed is 5.68 V/Å. This agrees with the value 5.7 V/Å obtained by others[2] for the (112) plane of tungsten.

DISCUSSION OF RESULTS: PARAMETERS OF FIELD EVAPORATION OF ATOMS FROM THE (112) FACE

To obtain quantitatively the values of certain parameters that characterize the field-evaporation process, we determined from the experimental data (Table I) by least squares[22] the coefficients $A_{0,1,2}$ and $A'_{0,1,2}$ in the expressions

$$\ln \frac{k_{ev}(F)}{k_{ev}(F_{ev})}=A_0+A_1F^{1/2}+A_2F^2, \quad (2)$$

$$\ln \frac{k_{ev}(F)}{k_{ev}(F_{ev})}=A_0'+A_1'F+A_2'F^2. \quad (3)$$

Both expressions correspond to the models (theories) most widely used at present for field evaporation. The first corresponds to model I, based on the image-force concepts,[4] and the second on the so-called charge-exchange model (model II).[25] Knowledge of the coefficient A_1 in the first expression makes it possible to determine the charge n of the evaporated ion ($A_1=(ne)^{3/2}$), and A_2 is the difference between the polarizability of the surface atom α_a and that of the evaporated ion α_i, i.e., the effective polarizability α_{eff} ($Z_2=\alpha_{eff}/2$). Assuming validity of the second model, the coefficient A_1' is used to determine the sum of the distance x_k, from the surface on which field evaporation takes place, and the depth of penetration λ of the field into the metal [$A'=ne(x_k+\lambda)$], while the value of A_2' is used to determine the effective polarizability α_{eff} ($A'=\alpha_{eff}/2$). The values of the parameters calculated in this manner are listed in Table II. For comparison with it, in addition, we present the analogous results of Ref. 24. The values of F_k in the last column of the table, likewise obtained from an analysis of expressions (2) and (3), correspond to the maximum rate k_{ev} of field evaporation.

We note that equations such as (2) and (3) can be made more accurate[8,25]: allowance for the additional terms in them yields a smaller value of $x_k+\lambda$ than obtained in the present paper.

As seen from Table II, the polarizability of the atoms on the edges of the (112) planes is substantially lower than for the {011} planes. Recognizing that the field penetrates less in the metal in the region of the {112} planes (the upper atoms of such planes are more strongly screened by the planes beneath them), this result is fully acceptable.

As for the existence of a certain critical value of the electric field intensity F_k, at which the evaporation rate k_{ev} reaches a maximum (we note that this is not contradicted by either of the indicated field-evaporation models), it must be stated that a direct experimental analysis of the kinetics of the field evaporation in fields of such a high intensity is extremely difficult. The reason is that the mechanical stresses that develop in the sample material in such fields becomes comparable with ultimate strength σ_{ult} of the tungsten tips ($\sigma_{ult}\approx 1950$ kg/mm^2, Refs. 26 and 27, corresponding to $F\approx 6.63$ V/Å).

The data obtained in the present paper on "collective" evaporation of atoms by a field when the upper plane reaches a definite size (see also the results of Mikhailovskiĭ *et al.*[11]) confirm, on the one hand, the conclusion[9] that metastable atom configurations exist, and suggest, on the other, a noticeable influence of the

TABLE II.

Model	Calculated value of n	Ion charge assumed in the calculation	$x_k+\lambda$, Å	α_e, Å^3	F_k[B/Å] / $\sigma(F_k)$ [kg/mm^2]
		(112) plane			
I	–	1	–	1.98	6.1635 / 1682.9
II	1	–	1.29	3.0	6.1648 / 1683.6
	2	–	0.64	–	–
	3	–	0.43	–	–
		(110) plane according to Ref. 24			
I	2	–	–	4.73	–
	3	–	–	9.09	–
II	2	–	1.27	5.56	6.5528* / 1902.6
	3	–	0.84	–	–
I	2	–	–	4.81	–
	3	–	–	9.13	–
II	2	–	1.04	4.58	6.5380* / 1893.6
	3	–	0.69	–	–

*Values calculated by the present authors in accord with the data of Ref. 24.

dipole-dipole interaction (repulsion) of the surface atoms within the confines of each of the plane in the course of field evaporation. The noticeable role of the dipole-dipole repulsion is indicated by the results of an analysis of the "last" (few remaining) atoms of the upper {111} planes of gold.[28] These atoms, before evaporating, aligned themselves in a chain along the close-packed directions ⟨110⟩. Their behavior during the field evaporation on the upper {110} planes of tungsten was investigated in Refs. 29 and 30. It was observed that clusters of the "last" atoms of the plane, when the sample was heated in the presence of an electric field (of the order of 0.75 of the best-image field), were drawn out in a chain along the [110] direction. When the sample with the chain of atoms was heated in the absence of the electric field, the chains again became bunched. This behavior of the atoms on the plane shows that at the best-image voltage the dipole-dipole interaction forces differ insignificantly from the interatomic-interaction forces in the plane. However, as seen from Eqs. (2) and (3), when the field intensity is increased the dipole-dipole interaction forces should play a more important role in field evaporation. The indicated increase of the mutual repulsion of the atoms decreases their screening and increases the field-evaporation probability. In a certain limiting case ($F \sim F_k$) the atoms of the upper plane of this type can move apart strongly. On reaching the edge of the second plane (beneath them) they are either ionized and evaporated by the field or else move away the plane (without being ionized) in a neutral state. It is just this type of evaporation that can explain certain peculiarities in the contrast of field-ion emission images (e.g., the "double edges" of the imaged atoms in the region of certain poles of the tungsten surface[6] at a temperature 21 K).

Figure 1 shows the field-ion images of the surface of a tungsten sample, obtained in continuous field evaporation at $T_0 = 78$ K and $F \approx 5.62$ V/Å. The observed dark regions in the center of the plane at the center of the {011} planes can be attributed to the "flying apart" of the atoms of the upper plane to the edges of the lower (second from the top) plane into the location of their evaporation. The distinctive annular structure of the planes is indirect confirmation of the existing of metastable atom configurations.[9,10] The second case-field evaporation of a tungsten sample in the continuous regime at $T_0 = 78$ K and $F \approx 5.9$ V/Å, is illustrated by the image of Fig. 2b, which has the appearance of the negative of the initial image ($F = 4.4$ V/Å) of Fig. 2a. The dark strips on Fig. 2b coincide with the directions most favorable for the migration of the surface atoms. It appears that the dipole-dipole interaction (repulsion) leads in the fields of the indicated intensity to dispersal of the surface atom in precisely these directions. The foregoing, is a partial explanation, in our opinion, also for the contrast of the micrograms obtained in a sublimation ion microscope[31] for field-evaporated ions of the sample itself.

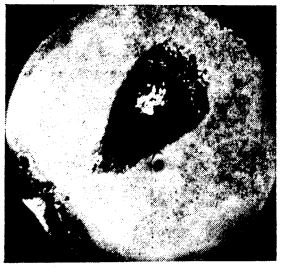

FIG. 1. Field-ion image of a tungsten surface containing a depleted zone, illustrating the kinetics of field evaporation in the continuous regime in a field $F \approx 5.62$ V/Å. ($U_0 = 20.0$ kV).

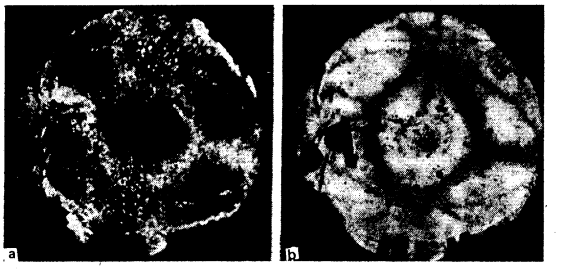

FIG. 2. Field-ion images of the same tungsten surface in fields 4.4 V/Å ($U_0 = 18.5$ kV) (a) and 5.9 V/Å ($U_0 = 24.0$ kV). Image b reflects the kinetics of high-speed continous field evaporation of the sample material.

PULSED FIELD EVAPORATION OF SAMPLES WITH DEFECTS

The main experiments were performed on thoriated tungsten samples irradiated by fast neutrons together with thorium-fission fragments,[32] as well as on samples of commercially pure tungsten bombarded by low-energy helium ions in the field-ion microscope itself with the high-voltage polarity reversed (by the technique described, for example, in Ref. 33). In both cases the temperature of the samples during the investigation was 78 K. When speaking of identification of solitary point defects on field-ion images of irradiated samples, we must emphasize above all an important specific feature of these experiments, namely that the observation of atoms shifted into interstitial positions is made possible in these experiments exclusively on account of stabilization on the impurity-element atoms,[34] inasmuch as long-range migration of interstitial atoms takes place in high-purity tungsten already at 38 K (Ref. 35), while at 100 K the overwhelming majority of these atoms emerges to the surface of the sample or is annihilated by the vacancies and their complexes encountered in the migration path. Thus, the brighter spots on ion-micrograms might be attributed either to interstitial atom + impurity atom complexes, or to atoms adsorbed on the surface of the tip during the time of various manipulations of the tip. Field evaporation of the tip material in the continuous regime, undertaken to study deep layers of the crystal lattice, remove both types of formation and make it impossible to distinguish between them. Moreover, in the case of adsorbed atoms, it can lead (as can, incidentally, also pulsed evaporation by a field) to formation of artificial vacancies by removing the adsorbed atoms jointly with the surface atoms of the tungsten sample (this was indicat-

ed also by the authors of Ref. 36). In pulse field evaporation, however, comparison of closely-exposed ion-emission images yields information on the cause of the vacancy, on the surface of the sample, corresponding to the "second" image (a dark spot appears at the location of the brighter spot), whereas in the case of continuous evaporation there is no such information. In addition, it was observed that interstitial atom + impurity atom complexes, at equal values of Δt, need an evaporating pulse of larger amplitude to remove them from the surface than adsorbed impurities. Therefore, by constantly increasing the value of ΔU we succeeded in distinguishing between the contrasts due to the presence of an interstitial atom and an adsorbed particle (using the so-called "rocking potential" method[37]).

In identification of vacancies and their small complexes (with not more than 10 components), pulsed field evaporation made it possible to separate the decrease of the image brightness of individual atoms of individual atoms that "cover up" a vacancy in the second layer from the surface[38] from the case when the vacancy is actually present in the imaged upper atomic layer, i.e., in particular, to distinguish unambiguously between an artificial vacancy and a true divacancy. This was accomplished by analyzing a sequence of pulse-evaporated atoms of the packed upper planes of definite crystal faces. It is clear that such a procedure (which is undoubtedly more laborious than analysis in the regime of continuous layer-by-layer evaporation of the sample material by the field) is needed also for the establishment of the point structure of the depleted zones. The latter, incidentally, are resistant to pulsed evaporation by a field (they do not deteriorate into pores, as is the case with continuous field evaporation[17,39]), even at relatively high vacancy concentration in them. This fact is illustrated by the sequence of field ion images of the surface of an irradiated tip in Fig. 3.

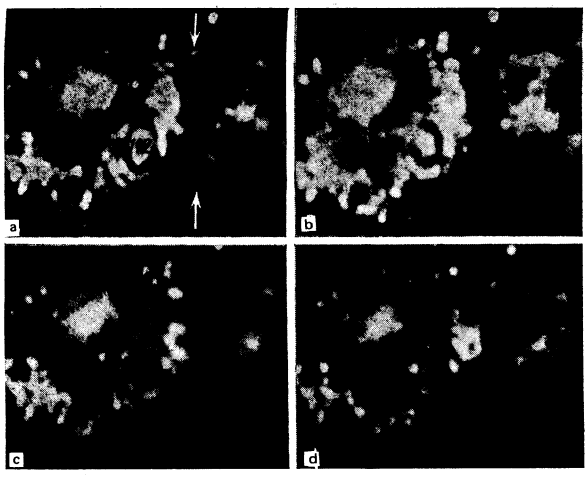

FIG. 3. Kinetics of pulsed field evaporation of sample of thoriated tungsten bombarded by fast neutrons and fission fragments. a) Initial image; b) after applying single evaporating pulses of duration $\Delta t = 0.1$ μsec and amplitude $\Delta U = 1.4$ kV; c) $\Delta t = 2.0$ μsec, $\Delta U = 2.8$ kV; *d*) $\Delta t = 0.2$ μsec, $\Delta U = 0.72$ kV. For all images, $U_0 = 14.0$ kV. The use of pulsed field evaporation makes it possible to avoid the erosion of the analyzed depleted zone (indicated by arrows in image a).

We have carried out here a comparative analysis of the results of field evaporation of a sample containing a pore, in both the continuous and the pulsed regime (the comparison, naturally is not absolute), inasmuch as in different cases we analyzed different sections of a pore on a sample surface bared by the field. As expected, pulsed field evaporation practically preserved the initial configuration of the pore (its edge hardly shifted from image to image in certain cases), whereas even a short-duration (several seconds) evaporation of the sample material by a continuously applied field led, in the overwhelmingly majority of cases, to a noticeable increase of the dimensions of the pore cross section in the image of the sample surface.

We note in conclusion that the very kinetics of field evaporation of atoms on the edge of a pore, just in the region of a depleted zone, can be a source of more detailed information on the point (atomic) structure of these defects; to take this information into account, however, it is necessary to have an analysis of the concrete crystallography of the sample and of the local distribution of the field on its surface, which of necessity calls for computer calculations.

[1]E. W. Müller, Phys. Rev. **102**, 618 (1956).
[2]T. T. Tsong, Surface Science **70**, 211 (1978).
[3]E. W. Müller and T. T. Tsong, Field Ion Microscopy, Am. Elsevier, 1969.
[4]E. W. Muller and T. T. Tsong, Progress in Surface Science, Pergamon Press, Vol. 4, (1974).
[5]T. T. Tsong and E. W. Müller, Phys. Stat. Sol. (a) **1**, 513 (1970).
[6]T. Adachi and S. Nacamura, Surface Science **59**, 61 (1976).
[7]A. J. W. Moore and J. A. Spink, *ibid.* **44**, 198 (1974).
[8]T. T. Tsong, J. Chem. Phys. **54**, 4205 (1971).
[9]A. L. Suvorov, T. L. Razikova, G. M. Kukavadze, A. F. Bobkov, B. Ya. Kuznetsov, and V. A. Kuznetsov, Zh. Eksp. Teor. Fiz. **68**, 1460 (1975) [Sov. Phys. JETP **41**, 729 (1975)].
[10]A. L. Suvorov, G. M. Kukavadze, D. M. Skorov, A. F. Bobkov, B. Ya. Kuznetsov, B. A. Kalin, V. B. Volkov, and S. V. Zaĭtsev, At. Energ. **38**, 72 (1975).
[11]I. M. Mikhailovskiĭ, Zh. I. Dranova, V. A. Ksenofontov, and V. B. Kul'ko, Zh. Eksp. Teor. Fiz. **76**, 1309 (1979) [Sov. Phys. JETP **49**, 664 (1979)].
[12]A. L. Suvorov and T. K. Razinkova, Surface Science **65**, 354 (1977).
[13]E. W. Müller, Transl. in: Metodika analiza poverkhnostei (Surface Analysis Technique). Mir, 1979, Chap. 8, p. 401.
[14]A. L. Suvorov and V. V. Trebukhovskiĭ, Usp. Fiz. Nauk **107**, 657 (1972) [Sov. Phys. Usp. **15**, 471 (1973)].
[15]D. N. Seidman and K. H. Lie, Acta Metallurgica **20**, 1045 (1972).
[16]A. L. Suvorov and A. G. Sokolov, Kristallografiya **17**, 1200 (1972) [Sov. Phys. Crystallogr. **17** 1052 (1973)].
[17]A. L. Suvorov and A. G. Sololov, *ibid.* **20**,379 (1975) [**20**, 232 1975)].
[18]A. L. Suvorov and A. G. Sokolov, Preprint ITEF-30, 1973 (Inst. of Theoretical and Experimental Physics).
[19]A. F. Bobkov, V. T. Zabolotnyĭ, L. I. Ivanov, and A. L. Suvorov, Voprosy atomnoĭ nauki i tekhniki, ser. fizika radiatsionnyk povrezhdeniĭ radiatsionnoe materialovedenie (Problems in Atomic Science and Engineering, series on Physics of Radiation Damage and Radiation Material

Science), Khar'kov, No. 1 (3), p. 26, 1976.
[20]A. L. Suvorov and T. L. Razinkova, Kristallografiya **20**, 599 (1975) [Sov. Phys. Crystallogr. **20**, 366 (1975)].
[21]A. L. Suvorov, Usp. Fiz. Nauk **101**, 21 (1970) [Sov. Phys. Usp. **13**, 317 (1970)].
[22]J. Matthews and R. Walker, Mathematical Methods of Physics, Russ. transl. Atomizdat, 1972.
[23]R. Gomer and L. W. Swanson, J. Chem. Phys. **38**, 1613 (1963).
[24]M. Yesely and G. Ehrlich, Surface Science **34**, 547 (1973).
[25]N. D. Lang and W. Kohn, Phys. Rev. B **7**, 3541 (1973).
[26]R. I. Garber, Zh. I. Dranova, and I. M. Mikhaĭlovskiĭ, Dolk. Akad. Nauk SSSR **174**, 1044 (1967) [Sov. Phys. Doklady **12**, 585 (1967)].
[27]A. L. Suvorov, G. M. Kukavadze, D. M. Skorov, B. A. Kalin, A. F. Bobkov, V. A. Fedorchenko, B. V. Sharov, and G. N. Shishkin, At. Energ. **38**, 412 (1975).
[28]E. D. Boyes and M. J. Southon, Vacuum **22**, 447 (1972).
[29]M. Audiffren, P. Traimond, J. Bardon, and M. Drechsler, Surface Science **75**, 751 (1978).
[30]S. Nishigaki and S. Nakamura, Japan J. Appl. Phys. **14**, 769 (1975).
[31]B. J. Walko and E. W. Müller, Phys. Stat. Sol. (a) **9**, K9 (1972).
[32]A. L. Suvorov, G. M. Kukavadze and A. F. Bobkov, in: Raktornoe materialovedenie (Reactor Material Science), TsNIIAtom Inform, 1978, Vol. 3, 143.
[33]J. M. Walls, E. M. Bothby, and H. N. Southworth, Surface Science **61**, 419 (1976).
[34]P. A. Bereznyak, R. I. Garber, V. S. Geĭsherik, I. M. Mikhaĭlovskiĭ, L. I. Pivovar, G. D. Tostolutskaya, op. cit. 19, 1(1), p. 30, 1974.
[35]D. N. Seidamn, Surface Science **70**, 532 (1978).
[36]C. G. Chen and R. W. Balluffi, Acta Metallurgica **23**, 919 (1975).
[37]A. L. Suvorov, Usp. Fiz. Nauk **117**, 685 (1975) [Sov. Phys. Usp **18**, 983 (1975)].
[38]T. L. Razinkova and A. L. Suvorov, Preprint ITEF-48, 1974.
[39]G. M. Kikavadze, A. L. Suvorov, and B. V. Sharov, Fiz. Met. Metallov, **27**, 797 (1969).

Translated by J. G. Adashko

An exactly soluble one-dimensional model of the thermodynamics of a rigid polymer molecule

A. S. Kovalev, A. M. Kosevich, and M. L. Polyakov

Low Temperature Physicotechnical Institute, Academy of Sciences of the Ukrainian SSR
(Submitted 20 March 1980)
Zh. Eksp. Teor. Fiz. **79**, 1385–1393 (October 1980)

We construct the statistical thermodynamics of a polymer molecule in an exactly soluble one-dimensional model, which takes into account the rigidity of the macromolecule. We analyze the equation of state of the macromolecule under the action of external pressure. We show that at a fixed pressure the temperature dependence of the size of the region where the molecule is localized is nonmonotonic.

PACS numbers: 36.20. – r, 05.70.Ce

1. INTRODUCTION. THE MODEL

An important problem in the theory of polymer macromolecules is that of spatial structure of long molecular chains of the protein or nucleic acid type. If the rigidity against bending of such a molecule is sufficiently small, the usual theoretical model to describe its statistical thermodynamical properties reduces to replacing the macromolecule by a chain with freely linked units (monomers). Confined to a closed volume or put in a sufficiently deep potential well, such a flexible and sufficiently long chain forms at a finite temperature a globule with a maximum monomer density at its center.[1,2] Of course, the structure of the globule must strongly depend on the rigidity of the macromolecule.

In the present paper we consider the effect of the rigidity of the macromolecule on the structure of the globule in an extremely simple model which allows only two configurations for the disposition of neighboring monomers. They can form only a zero angle (being directed to the same side) or an angle π between them. These two configurations have different coupling energies, and this is the manifestation of the rigidity of the chain.

The description of the state of a macromolecule is then similar to the description of the one-dimensional wandering of a point, where the probability for the direction of the next step depends on the direction of the preceding step. The system, of the type of a folding rule, is arranged along a straight line which we choose for our x-axis. The macromolecule consists of monomers of equal length a, their joints are positioned on sites with discrete coordinates $x_n = an$ ($n = 0, \pm 1, \pm 2, \ldots$). It is convenient for us to describe the configuration of a chain in terms of the joints; therefore we introduce a numbering of the joints on the chain, starting at its beginning ($i = 0, 1, 2, \ldots$), and we define a parameter σ_i that specifies the state of the i-th joint. This parameter takes the values $\sigma_i = \pm 1$ and indicates the relative position of the preceding joint with respect to the given one: $x_i = x_{i-1} + a\sigma_i$. It is clear that the configuration of the chain is uniquely determined by the set $\{\sigma_i\}$. Indeed, if the start of the chain is at the point $x = 0$, we have

$$x_k = a\sum_{i=1}^{k}\sigma_i.$$

In the presence of an external field that acts upon the

 0038-5646/80/100699-05$02.40